Hemodynamic Changes after Occlusion of the Posterior Superior Sagittal Sinus: An Experimental PET Study in Cats

Bernhard Schaller, Rudolf Graf, Yasuhiro Sanada, Markus Tolnay, Gerhard Rosner, Klaus Wienhard and Wolf-Dieter Heiss

AJNR Am J Neuroradiol 2003, 24 (9) 1876-1880
http://www.ajnr.org/content/24/9/1876

Hemodynamic Changes after Occlusion of the Posterior Superior Sagittal Sinus: An Experimental PET Study in Cats

Bernhard Schaller, Rudolf Graf, Yasuhiro Sanada, Markus Tolnay, Gerhard Rosner, Klaus Wienhard, and Wolf-Dieter Heiss

BACKGROUND AND PURPOSE: **Occlusion of the anterior third of superior sagittal sinus (SSS) is generally well tolerated because of sufficient collateral venous blood flow. In contrast, the pathophysiologic effects of occlusion of the SSS posterior to the rolandic vein remain controversial. We aimed to identify the specific hemodynamic effects of this subtype of SSS occlusion.**

METHODS: **We ligated the SSS just behind rolandic vein and in the posterior part near the confluens sinus in three anesthetized cats. Regional cerebral blood flow (rCBF) was measured before and at 2 and 24 hours after the SSS occlusion. At around 48 hours, experimental settings were terminated with perfusion fixation with 4% paraformaldehyde solution. Hematoxylin-eosin histologic evaluation was performed.**

RESULTS: **In all three cats with SSS occlusion, rCBF was reduced over the time period of measurement; this finding was observed in areas covering 5–20% of the brain in planes affected by the occlusion. The degree of rCBF reduction and the extension and severity of histologically proved venous infarction were correlated.**

CONCLUSION: **To our knowledge, this is the first demonstration that occlusion of the SSS posterior to the rolandic vein is associated with a significant rCBF reduction to still-viable tissue in the related vascular territory at 24 hours after occlusion. We describe subacute venous infarction in an experimental occlusion of the SSS. Analogous to clinical conditions, occlusion of SSS alone without additional occlusion of bridging veins is adequate for producing a venous circulatory disturbance.**

Sinus venous occlusion is increasingly recognized as an important cause of focal neurologic deterioration, whether it is surgically induced by vascular-compressing mass lesions or by intrasinusal thrombosis. However, its underlying pathophysiologic pathways remain poorly understood (1–3). The development of ischemic damage to brain tissue seems to be different in venous occlusions compared with arterial occlusions (3). Experimental studies have provided evidence of not only short-term changes but also long-term alterations in intracranial pressure (ICP), regional cerebral blood flow (rCBF), neuronal function, and morphology after complete cerebral sinus or venous occlusion (1, 2). Only occlusion of the anterior third of the superior sagittal sinus (SSS) is generally accepted to be well tolerated, because of sufficient collateral venous blood flow via end-to-end anastomoses with the superficial cortical veins (4). Occlusion of the SSS posterior to the rolandic vein has been thought to induce an enhanced transmural pressure gradient with consecutive cerebral brain tissue edema and mass effect leading to venous infarction (5). Recommendations regarding a strategy to prevent or treat such sinus venous occlusion are still controversial (6). Therefore, it is important to study the pathophysiologic changes leading to venous infarction by using animal models. We present here what we believe is the first study of the hemodynamic effects investigated by means of sequential positron emission tomography (PET) before and after experimental occlusion of the posterior SSS.

Received March 6, 2003; accepted after revision April 24.

From the Max-Planck-Institute for Neurologic Research, Cologne, Germany (B.S., R.G., Y.S., G.R., K.W., W.-D.H.), and the Department of Neuropathology, Institute of Pathology, University Hospitals, Basel, Switzerland (M.T.).

Address reprint requests to R. Graf, PhD, Max-Planck-Institute for Neurologic Research, Gleueler Strasse 50, D-50931 Cologne, Germany.

Methods

Animal Preparation

Three adult male cats weighing 3.1–4.7 kg were anesthetized with ketamine hydrochloride (25 mg/kg) administered by means of intramuscular injection. The left femoral vein and

artery were catheterized to measure the mean arterial blood pressure (MABP) and to obtain samples for determining arterial blood gas, hemoglobin, and plasma glucose concentrations, as well as to administer drugs as necessary. A tracheostomy was performed; the animals were immobilized with 0.2 mg/kg pancuronium bromide and ventilated artificially. Generalized anesthesia was maintained by using 0.6–1.2% halothane in a mixture of 70% nitrous oxide and 30% oxygen gas. An intravenous infusion of Ringer solution 2 mL/kg/h containing gallamine triethiodide 5 mg/kg/h for muscle relaxation was maintained throughout the experiments. Physiologic variables were kept in the normal range known for awake cats (7). The animals' deep-body temperature was kept at 37°C by using a heating blanket feedback controlled via a rectal temperature probe. The present study was approved by the local animal care committee and the Regierungspräsident of Cologne, Germany, and it was performed in compliance with German laws for animal protection.

Immediately after induction of generalized anesthesia, a large, midline skin incision was made, followed by an additional *V*-shaped incision extending posteriorly. Subsequently, myocutaneous flaps were proposed and parasagittal craniectomies were performed on both sides: two burr holes of 3-mm diameter were drilled in the parietotemporal and temporo-occipital areas by using a dental high-speed drill (Bien Air, Surrey, UK). The parasagittal cortex with the intact overlying dura mater was exposed by widening these burr holes under microscopic control (Carl Zeiss, Inc, Jena, Germany) by using a rongeur. An osseous bridge was left intact above the SSS. Care was taken to avoid lesions of the sigmoid sinus and SSS (to prevent the possibility of sinus thrombosis). Small, 1–2-mm longitudinal cuts were made in the dura mater on both sides at the level of the burr holes. The SSS was snared first in the middle part just behind the rolandic vein and then in the posterior part close to the confluens sinus by using 9–0 Prolene, without damaging the adjacent brain tissue. Initially, the snare was not tightened but protected with a silicon tube. For continuous monitoring, an intracranial pressure measuring device was placed epidurally on the parietal part and zeroed to atmospheric pressure. The skull was substituted with a cranioplasty that was fixed without sealing the cranium by suturing the temporalis muscle and the skin flap in plane.

Experimental Protocol

Routine monitoring of physiologic parameters included measurements of the heart rate, MABP, rCBF and ICP. In addition, end-tidal concentration of CO_2 ($P_{ET}CO_2$; range, 3.5–4.5 kPa) and halothane ($P_{ET}HAL$; range, 0.8–1.2 kPa) were monitored by an infrared gas-analyzer (Datex, Helsinki, Finland). All parameters were continuously recorded by using a PC-based data-acquisition system (Dasy Lab; National Instruments).

PET images of rCBF were obtained before and around 2 and 24 hours after SSS occlusion, SSS occlusion was achieved by tightening the snare in the PET scanner.

At the end of each experiment, usually 48 hours after SSS occlusion, experiments were terminated by means of perfusion fixation with a 4% paraformaldehyde solution under general anesthesia. In each cat, the brain was carefully removed from the skull and embedded in paraffin.

PET Imaging

Serial PET imaging was performed with a 24-ring, high-resolution camera (CTI ECAT EXACT HR; Siemens, USA) with an axial field of view of 15 cm, an in-plane spatial resolution of 3.6 mm full width at half maximum, and an axial resolution of 4.0 mm full width at half maximum (8). Starting around 2 hours before SSS occlusion, several consecutive PET studies were performed in each cat. For the assessment of rCBF, bolus applications of ^{15}O-H_20 were used, as described and discussed before (8–14).

Analysis of the PET data was based on the parametric images of 14 coronal brain sections. The obtained images permitted the identification of the main anatomic structures of the cat's brain and a distinction of gray and white matter. For quantitative analysis, CBF images obtained during control were masked by using an CBF threshold of 10 mL/100 g/min to obtain images that represented the whole brain. These masks were used to analyze coronal brain sections in subsequent scans.

On coronal sections, regions with an rCBF threshold >30 mL/100 g/min were reconstructed by an exploratory tool that was used allowing voxel-by-voxel comparison as previously described in detail (15). In scatterplots, clusters of voxels were separated from the normal distribution of voxels by defining the threshold of >30 mL/100 g/min. The ratios between these regions of <30 mL/100 g/min and the whole sections were calculated. Furthermore, rCBF was determined in circular regions positioned in the center of the affected areas in respect to the coronal sections.

Histology

After paraffin embedding, 7-μm-thick coronal sections were cut at distances of 2 mm throughout the whole brain and stained with hematoxylin-eosin (HE) or with a combination of Luxol fast blue and cresyl violet. Each hemisphere of the tissue specimen was separately graded according to the four stages of histologic changes.

Infarct areas were determined by calculating areas with low-intensity staining on HE sections, by using a computer-interfaced image analyzer (Scion Image). The extent of infarction was calculated by dividing the areas of infarcted tissue in each hemisphere by the total area of the same hemisphere. Means of the percentage values of infarction were calculated for individual animals.

The histopathologic grades were defined as follows: stage 0 was defined as no parenchymal changes; stage I, mild edematous changes; stage II, moderate parenchymal edema and/or ischemic changes in neurons with or without small hemorrhages; and stage III, moderate-to-severe hemorrhage.

Statistical Analysis

Statistical analysis (StatSoft, Tulsa, OK) was performed by using a repeated-measures analysis of variance with a Scheffé post hoc comparison to test variation over time. Statistical significance was defined at $P < .05$.

Results

General Physiologic Parameters

Arterial blood gas levels, pH, hemoglobin concentrations and ICP in the three cats remained within normal physiologic limits throughout the experiments. Mean systemic arterial pressure was not significantly altered by the surgical procedure (occlusion of SSS), nor were changed in the later course of the experiments (all data not shown).

Histologic Data

Histopathologic light microscopic observations demonstrated subacute, focally extensive hemorrhagic necrosis, predominantly in the posterior third of the marginal gyrus. This finding was accompanied by eosinophilic hypoxic-ischemic neuronal death (Fig 1). Thrombotic material was always found within the occluded part of the SSS.

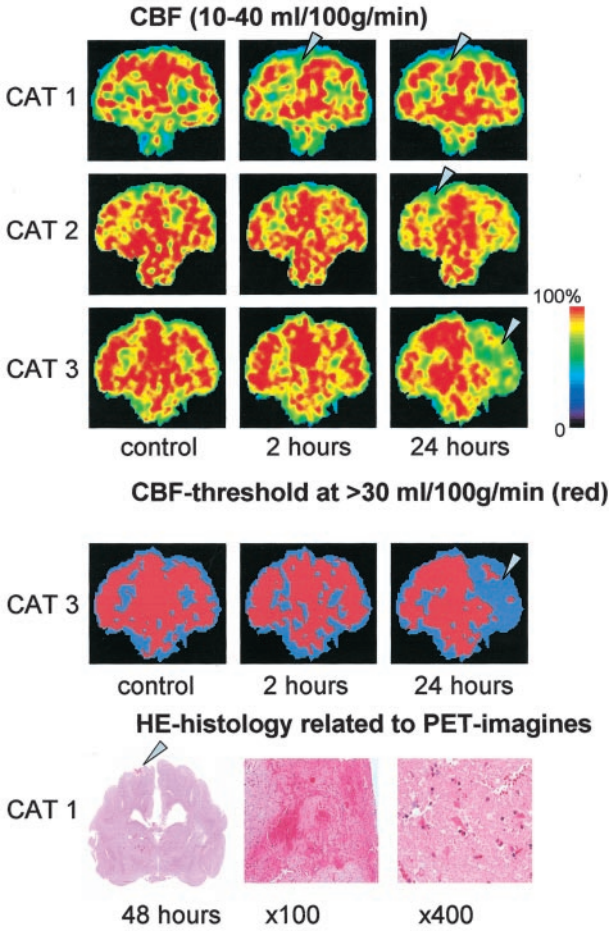

FIG 1. Representative PET images and histologic sections. *Top*, Sequential PET images of CBF obtained at control and at 2 and 24 hours after SSS occlusion. *Arrowheads* indicate regions of main decreased flow. *Middle*, rCBF thresholds on PET images at >30 mL/100 g/min (*red*). *Bottom*, Representative cross-sections of subacute hemorrhagic infarct (HE stain). Low-power view (original magnification ×100) shows subacute, focally extensive hemorrhagic necrosis accompanied by eosinophilic hypoxic-ischemic neuronal changes in the high-power view (original magnification ×400).

Histopathologic changes were classified as predominantly stage III (75%), related to the marginal gyrus, or predominantly stage 0 or I, related to the ecto-Sylvian or supra-Sylvian gyrus (Table 1). The quantitative assessment of the damaged brain tissue area, measured by using image analyzer, revealed the following results: cortical, 1.6%; subcortical, 0.96%; marginal, 2.2%; and ecto-Sylvian gyrus, 0.29%.

PET Measurements

Sequential multivariate PET scans obtained before and at approximately 2 and 24 hours after SSS occlusion are illustrated on the coronal sections shown in Figure 1. The experimental procedure significantly decreased the rCBF in the vascular territories related to the SSS occlusion.

Evaluation of the means in both hemispheres revealed that rCBF decreased in brain-tissue regions related to the SSS occlusion. Direct comparisons between regions affected and regions not affected demonstrated a decrease of rCBF to 20–30% in the affected center planes (cat 1, planes 8–12; cat 2: planes 7–9; cat 3: planes 6–11) (Table 2). The larger percentage decrease of rCBF in the circular regions reflected the more focused regional analysis.

Further data analysis of the PET parameters over time was focused on the circular regions of interest positioned in the center of the affected areas. This revealed significant reduction in the rCBF below 30 mL/100 g/min in cat 1 at 2 hours ($P < .05$) and in all three cats at 24 hours after SSS occlusion ($P < .05$). Consequently, the ratio in individual coronal sections between the size of the areas with a value of >30 mL/100 g/min and the areas of the whole brain in affected coronal brain sections decreased over time (Table 2). At 24 hours, this decrease was significant in cat 3 ($P < .05$). At histologic evaluation, this cat had the largest infarct with extensive perifocal edematous changes in most of the subcortical area of the related vascular territory.

When we compared the means of the regions of interest in the two hemispheres, the degree of rCBF

TABLE 1: Grouped summary of histologic changes after SSS occlusion posterior the rolandic vein

	Histologic Stage*			
Anatomic Location	0	I	II	III
Marginal gyrus				
Anterior third	75%	NA	25%	NA
Median third	NA	NA	75%	25%
Posterior third	25%	NA	NA	75%
Ecto-Sylvian gyrus	25%	75%	NA	NA
Supra-Sylvian gyrus	100%	NA	NA	NA

Note.—NA indicates not available. Data are the percentage of all cats' hemispheres that were histologically examined by using coronal sections (stained with HE).

* Stage 0 indicated no parenchymal changes; stage I, mild edematous changes; stage II, moderate parenchymal edema and/or ischemic changes in neurons with or without small hemorrhages; and stage III, moderate-to-severe hemorrhage. NA: not available.

TABLE 2: Summary of detailed rCBF data in all three cats

Data*	Control	At 2 h	At 24 h	Sum of Affected Coronal Sections
Cat 1				5
Ratio, %	70 ± 7	66 ± 8	64 ± 5	
CBF	44.1 ± 5.7	26.3 ± 8.7†	18.5 ± 6.8†	
Cat 2				3
Ratio, %	73 ± 6	71.8 ± 8	66 ± 9	
CBF	39.3 ± 8.4	32.8 ± 7.5	17.2 ± 7.0†	
Cat 3				6
Ratio, %	76 ± 5	73 ± 8	55 ± 14†	
CBF	46.2 ± 6.4	44.8 ± 8.4	20.1 ± 9.2†	

Note.—Values are mean ± SD.

* The ratio indicates the area with rCBF >30 mL/100 g/min as percentage of the area of the whole brain in affected coronal brain sections. CBF is reported in milliliters per 100 g per minute and was obtained in circular regions (mean, 8 mm) positioned in the center of affected areas on the coronal sections.

† $P < .05$; significantly different compared with control.

reduction was not uniform and demonstrated pronounced laterality. Individual infarcts, as well as their average sizes, were in good agreement with the PET regions of impaired rCBF (Fig 1). There was a relationship between the areas of reduced rCBF and the areas of infarction. From these data, it was obvious that histologically subacute infarction was slightly smaller than the area of reduced rCBF.

Discussion

In the present report, we provide what we believe is the first experimental evidence that occlusion of the SSS posterior to the rolandic vein may be associated with a reduction of rCBF in the related vascular brain tissue territory at 24 hours after occlusion. Therefore, analogous to clinical conditions, SSS occlusion alone without additional occlusion of bridging veins is capable of producing a notable circulatory disturbance.

On the basis of the presented data, we suggest that all three cats developed a collateral venous pathway after SSS occlusion. It may be expected that the opening of the end-to-end anastomosis of the meningeal veins to other venous channels preserves a functioning vascular drainage system, but this process demonstrates great interindividual and interhemispheric variations (16). This concept is best exemplified by the only-gradual onset of the hemodynamic changes and the pronounced laterality of the rCBF reduction in the present experiments. We assume that the gradual decrease of rCBF was induced by an elevation of venous pressure rather than by an increase in ICP. Wagner and Traystman (17) examined the rCBF response to elevated jugular venous pressure and found that rCBF decreased significantly when cerebral perfusion pressure decreased to values below 60 mm Hg. Intrasinusal venous hypertension undoubtedly plays an important role in the pathophysiology of venous hemorrhage and brain-tissue edema. It produces intracerebral venous congestion, increases intravascular pressure, and lowers the cerebral perfusion pressure (3). These pathophysiologic factors lead to complicated and potentially dangerous clinicopathologic events under these special conditions of the cerebrovenous circulation (18). The pathophysiologic character and magnitude of the responses may resemble prolonged cerebral arterial ischemia (2). For this reason, large areas of only transiently and reversibly disturbed brain tissue can be found after sinus venous occlusion. These resemble ischemic penumbra, as seen in the present study at 24 hours after SSS occlusion. If, however, venous occlusion is maintained for longer time periods, the described "meta-stable" areas may become necrotic, as shown with histologic analysis after SSS occlusion. Venous hemorrhage, predominantly located in parasagittal subcortical white matter, is considered to be the final consequence in the pathologic process and may develop, depending on the degree of intrasinusal venous pressure distal to the occlusion site and on the time interval from venous occlusion. The factor of the time interval is documented in the present experimental series; the factor of intrasinusal venous pressure is part of the surgical experience in monitoring the intrasinusal pressure (18, 19).

The presented results are clinically relevant, as they indicate that the pathophysiologic mechanisms of venous infarction differ from those of arterial ischemic damage. Determination of the extent to which aggressive (clinical) treatment option should be pursued remains controversial in dural sinus occlusion—contrary to arterial occlusion—as a consequence of its variable natural history. However, the present results show that the time window of effective treatment is presumably longer in cerebral venous occlusion than the reported 3–6 hours for cerebral arterial occlusion. Our data may help to define such a time window on a pathophysiologic basis, underlining the clinical hypothesis that treatment may be meaningful for up to 24 hours (20). Perhaps more importantly, our results may have implications on surgical procedures, such as skull-base operations, that pose risks for ischemic complications in normal brain tissue after intraoperative (transient) occlusion of the posterior part of the SSS. Possible deleterious effects of such interventions may partly be explained by hemodynamic effects like those described in our study, but they may be less frequent than previously expected, as our PET results demonstrated at 2 hours after SSS occlusion. From the present study, it may be speculated that an intermittent (<24-hour) occlusion of the SSS behind the rolandic vein, in cases of preserved collateral pathways, may be possible without persistent ischemic damage to brain tissue.

Conclusion

We have demonstrated that occlusion of the SSS behind the rolandic vein produces a gradual decrease of rCBF at 24 hours, leading to subacute venous infarction. Further experimental and clinical studies are needed to shed more light on the pathophysiologic basis of the phenomena found in the present study.

Acknowledgments

The authors thank Ms D. Lattacz, Ms C. Kleineberg, Ms C. Selbach, Mr A. Beyrau, and Dipl. Ing. B. Rademacher for their excellent technical assistance.

References

1. Ungersböck K, Heimann A, Kempski O. **Cerebral blood flow alterations in a rat model of cerebral sinus thrombosis.** *Stroke* 1993 24:563–570
2. Frerichs KU, Deckert M, Kempski O, et al. **Cerebral sinus and venous thrombosis in rats induces long-term deficits in brain function and morphology: evidence for a cytotoxic genesis.** *J Cereb Blood Flow Metab* 1994;14:289–300
3. Miyamato K, Heimann A, Kempsi O. **Microcirculatory alterations in a Mongolian gerbil sinus-vein thrombosis model.** *J Clin Neurosci* 2001;8(Suppl 1): 97–105
4. Oka K, Rhoton AL Jr, Barry M, et al. **Microsurgical anatomy of the superficial veins of the cerebrum.** *Neurosurgery* 1985;17:711–748

5. Longue V. **Parasagittal meningiomas.** In: Krayenbühl H, ed. *Advances and Technical Standards in Neurosurgery.* Vol 1. Berlin: Springer-Verlag; 128–141
6. Einhaupl KM, Villringer A, Meister W, et al. **Heparine treatment in sinus venous thrombosis.** *Lancet* 1991;338:597–600
7. Herbert DA, Mitchell RA. **Blood gas tensions and acidic balance in awake cats.** *J Appl Physiol* 1971;30:434–436
8. Wienhard K, Dahlbom M, Eriksson L, et al. **The ECAT EXACT HR: performance of a new high resolution positron scanner.** *J Comput Assist Tomogr* 1994;18:110–118
9. Baron JC, Frackowiak RSJ, Herholz K, et al. **Use of PET methods for measurement of cerebral energy metabolism and hemodynamics in cerebrovascular disease.** *J Cerebr Blood Flow Metab* 1989;9: 723–742
10. Eriksson L, Holte S, Bohm C, et al. **Automated blood sampling systems for positron emission tomography.** *IEET Trans Nucl Sci* 1988;35:703–704
11. Heiss WD, Graf R, Wienhard K, et al. **Dynamic penumbra demonstrated by sequential multitracers PET after middle cerebral artery occlusion in cats.** *J Cereb Blood Flow Metab* 1994 14:892–902
12. Herscovitch P, Markham J, Raichle ME. **Brain blood flow measured with intravenous H_2-^{15}O, I: theory and error analysis.** *J Nucl Med* 1983;24:782–789
13. Mintun MA, Raichle ME, Martin WRW, et al. **Brain oxygen utilization measured with 015 radiotracers and positron emission tomography.** *J Nucl Med* 1984;25:177–187
14. Reivich M, Kuhl D, Wolf A, et al. **The (^{18}F) fluorodeoxyglucose method for the measurement of local cerebral glucose utilization in man.** *Circ Res* 1979; 44:127–137
15. Graf R, Schuster A, Löttgen J, et al. **Sequential experimental PET: Voxel-based analysis reveals spatiotemporal dynamics of perfusion in transient focal cerebral ischemia.** In: Carson RE, Daube-Witherspoon ME, Herscovitch P, eds. *Quantitative Functional Brain Imaging with Positron Emission Tomography*. San Diego: Academic Press; 1998:145–149
16. Jacobs K, Moulin T, Bogousslavsky J, et al. **The stroke syndrome of cortical vein thrombosis.** *Neurology* 1996;47:376–382
17. Wagner EM, Traystman RJ. **Effects of cerebral venous and cerebrospinal fluid pressure on cerebral blood flow.** In: Auer LM, Lowe F, eds. *The Cerebral Veins.* New York: Springer-Verlag; 223–230
18. Sekhar LN, Chanda A, Morita A. **The preservation and reconstruction of cerebral veins and sinuses.** *J Clin Neurosci* 2002;9:391–399
19. Kanno T, Kasama A, Shoda M, et al. **Intraoperative monitoring on the occlusion of the venous system.** *Neurosurgeon (Jpn)* 1992;11: 51–59
20. Frey JL, Muro GJ, McDougall CG, et al. **Cerebral venous thrombosis: combined intrathrombus rtPA and intravenous heparin.** *Stroke* 1999;30:489–494